EJB Electronic Journal of Biotechnology ISSN: 0717-3458

Vol.1 No.2, Issue of August 15, 1998.
Received for review July 22, 1998

RESEARCH ARTICLE

Molecular modeling of manganese peroxidase from the lignin-degrading fungus *Ceriporiopsis subvermispora* and structural comparison with other peroxidases

Mauricio Canales [1]
Laboratorio de Biofísica, Facultad de Ciencias Biológicas, Universidad de Concepción. Casilla 152-C, Correo 3. Concepción, Chile. Tel.: (56 41) 234985, Ext. 2587; Fax (56 41) 245975;
E-mail: mcanale@udec.cl

Sergio Lobos
Facultad de Ciencias Químicas y Farmacéuticas, Universidad de Chile. Casilla 174, Correo 22. Santiago, Chile.

Rafael Vicuña
Departamento de Genética Molecular y Microbiología, Facultad de Ciencias Biológicas, Pontificia Universidad Católica de Chile. Casilla 114-D. Santiago, Chile.
E-mail : rvicuna@genes.bio.puc.cl

***Ceriporiopsis subvermispora* is a white-rot basidiomycete that produces several isoenzymes of manganese peroxidase (MnP). A cDNA of one of them (MnP13-1) has been isolated and sequenced. The deduced aminoacid sequence shows about 60% similarity with the MnPs from *Phanerochaete chrysosporium*. Based on the crystal structures of MnP and lignin peroxidase (LiP) from *P. chrysosporium*, and of a peroxidase from *Arthromyces ramosus* (ARP), we have modeled by homology the three dimensional structure of MnP13-1 using standard modeling procedures. Local molecular mechanics optimization performed in the region corresponding to the binding sites of Ca^{2+} and Mn^{2+} in MnP13-1 demonstrated that the stereochemistry and the geometry of binding are conserved in both MnPs. A putative aromatic binding site in MnP13-1 is described. We also report structural differences between the two MnPs, arising from the insertion in MnP13-1 of the sequences TGGN between residues S230 and D231 and TDSP at the C-terminal, both of which may have functional significance.**

The white-rot basidiomycete *Ceriporiopsis subvermispora* is strongly ligninolytic (Otjen et al. 1987, Blanchette et al. 1992). When growing on wood chips or in agitated liquid cultures, this fungus produces several isoenzymes of manganese-dependent peroxidase (MnP) and laccase (Lobos et al. 1994, Salas et al. 1995). We have characterized some isoenzymes of MnP with respect to substrate specificity and requirement of Mn^{2+} for activity (Urzúa et al. 1995), and recently we have isolated a cDNA clone of one of them (MnP13-1, GeneBank Access # U60413). The amino acid sequence deduced from the cDNA is over 60% homologous to the published MnP sequences from *P. chrysosporium* (Pribnow et al. 1989, Mayfield et al. 1994, Alic et al. 1997), although MnP13-1 is 7 to 9 amino acids longer (Lobos *et al.*, manuscript in preparation). Consistent with the peroxidase mechanism of MnP, the proximal and distal histidines and the distal arginine of MnP13-1 are all conserved, whereas regions flanking these residues display homology with other peroxidases, including manganese binding sites E35 and E39. The motif L/V/I-P-X-P, assigned as an aromatic binding site (Veitch 1993), shares also high homology with other peroxidases, although it is less hydrophilic.

MnPs from *C. subvermispora* are able to oxidize aromatic compounds in the absence of Mn^{2+} (Urzúa et al. 1995). This suggests direct binding of the substrate as it occurs with LiP, which possesses a pocket near the hem for the binding of veratryl alcohol (Poulos et al. 1993). To gain insight into this singular property of MnPs from this fungus, we have modeled MnP13-1 by homology based on the crystal structures of LiP and MnP from *P. chrysosporium*, and of a peroxidase from *Arthromyces ramosus* (ARP). A comparison between this model with the common folding of known peroxidases with emphasis on MnP from *P. chrysosporium* revealed some unique features of MnP13-1. The structural role of insertions in MnP13-1 and some properties of a putative aromatic binding site are discussed with respect to their possible effects on the mechanism of this enzyme.

Materials and Methods

Crystal structures of LiP from *P. chrysosporium* solved to 2.03 Å resolution (Poulos et al. 1993) and to 2.6 Å resolution (Edwards et al. 1993), of MnP from *P. chrysosporium* solved to 2.06 Å resolution (Sundaramoorthy et al. 1994) and of a peroxidase from *Arthromyces ramosus* (ARP) solved to 1.9 Å resolution (Kunishima et al. 1994) were used as reference. Structural alignment was done by calculation of Cα distance matrices and by computing the RMSD between boxes of equal length in proteins. The algorithm implemented in Homology from Biosym/MSI was employed.

The enhanced Needleman and Wunsch algorithm for pairwise comparison was used for sequence alignment (Needleman and Wunsch 1970). Local and global optimization of modeled proteins was done by AMBER parametrized according to recent developments (Pearlman et al. 1991). The modeling procedure was that of Greer (Greer 1981) and Blundell et al. 1987), described for the alignment of more than one known crystal structure. Testing of the model quality was conducted by comparing both the geometry and the stereochemistry with the crystal structure of the MnP reference. The optimization of ion binding sites was done taking the ion coordinates from the MnP reference and keeping fixed their positions during all the optimization steps. Ligand residues were optimized without restrain.

[1] **Corresponding author**

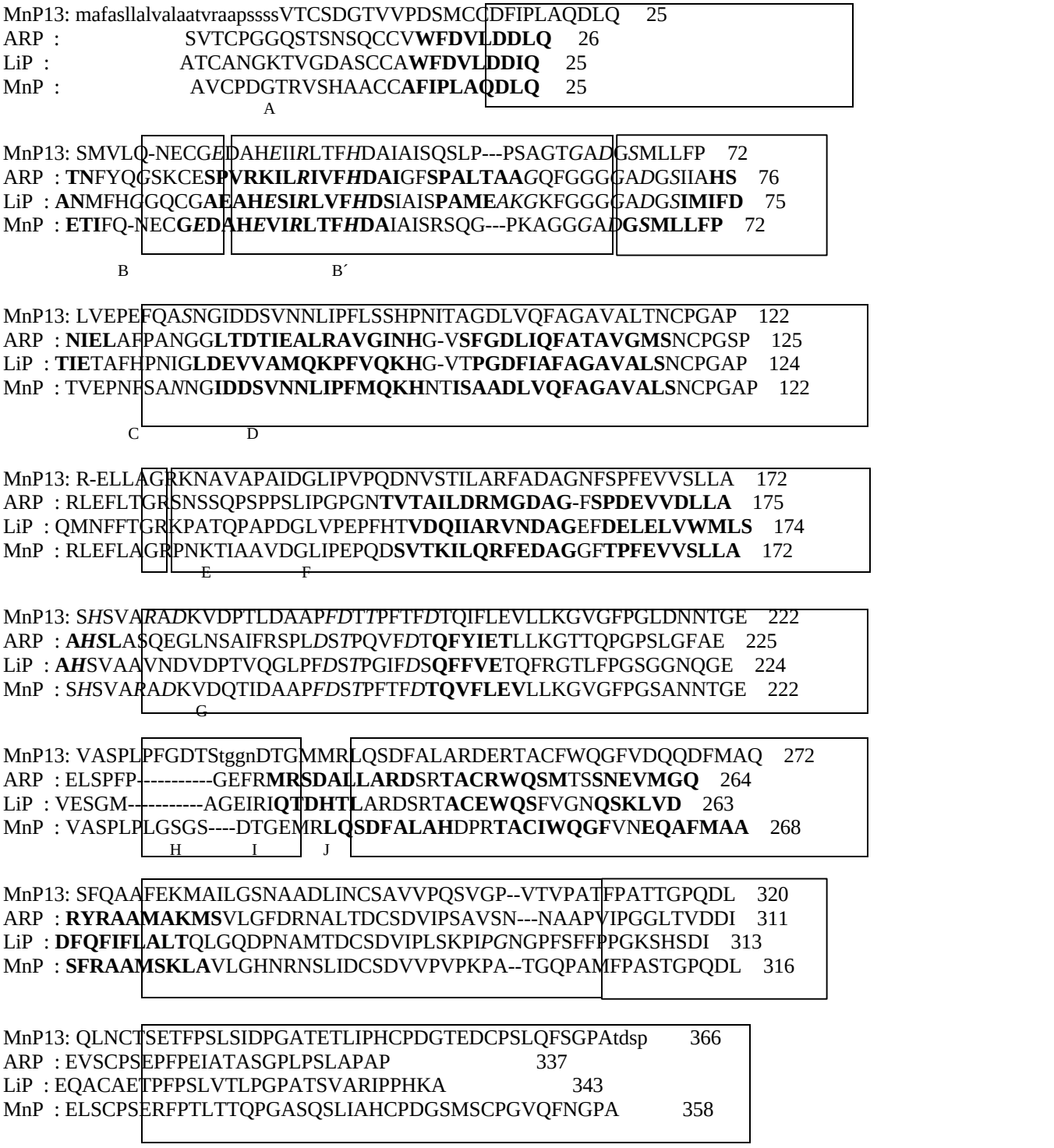

Figure 1. Sequence alignment of MnP13-1 from *C. subvermispora* (in this Fig. MnP13) with ARP, LiP and MnP. Dark letters indicate the localization of a -helix structures (A-J). Residues important for enzyme function are shown in italics. Boxes indicate structurally conserved regions.

Results

Structural comparison between ARP, LiP and MnP and sequence alignment with MnP13-1

An overall deviation of 0.96 Å /res was obtained after overlaping of mainchain atoms of the reference enzymes ARP, LiP and MnP. In agreement with previous reports (Henrissat et al. 1990) the RMSD matrix between these proteins shows a closer relation between LiP and MnP (0.85 Å /res), than between ARP and LiP (1.00 Å /res) or ARP and MnP (1.00 Å /res). Seven and eight boxes of conserved regions were calculated (see Methods), considering the secondary structure of the proteins (Fig. 1). Thereafter, MnP13-1 sequence was aligned over the reference structures

and from the scores obtained (Table 1), the overall similarity of both MnPs is evident. Only box 3 of LiP showed a score slightly greater (38.3) than the corresponding score for box 4 of MnP from *P. chrysosporium* (37.7). However, the latter encompasses over 65 residues, whereas box 3 from LiP contains only 22 residues.

An unexpected lower score was obtained for segments E148-G183 (box 4) and R266-P327 (box 7), showing more similarity of MnP13-1 to ARP than to LiP. The former segment embodies the helix E of ARP and MnP and the helix 7A of LiP.

Table 1. Structurally conserved regions and scores of similarity for MnP13-1*

Box Nº	Residues	Scores ARP	Scores LiP	Residues	Scores MnP
				V25-S29 A1-P4	32.5
				D30-Q55 D5-Q30	36.5
1	V25-P82 V10-A67	14.3	21.0	N56-P81 N31-G56	39.2
2	S83-P123 F71-G111	14.1	21.2		
3	I125-R147 V112-R134	36.9	38.3	P82-R147 R57-R122	37.7
4	E148-G183 E136-G171	24.7	22.8		
5	F185-P251 F172-P238	20.7	24.5	F148-S25 E124-S232	37.2
6	G253-T255 G239-F241	16.7	26.7		
7	R266-P327 R242-N303	25.6	24.5	D261-P327 D233-A299	34.2
8	T329-C369 N304-P344	16.6	13.4	V328-A385 T300-A357	36.4

* The upper numbers correspond to the reference proteins, whereas the numbers below correspond to the MnP13-1 sequence

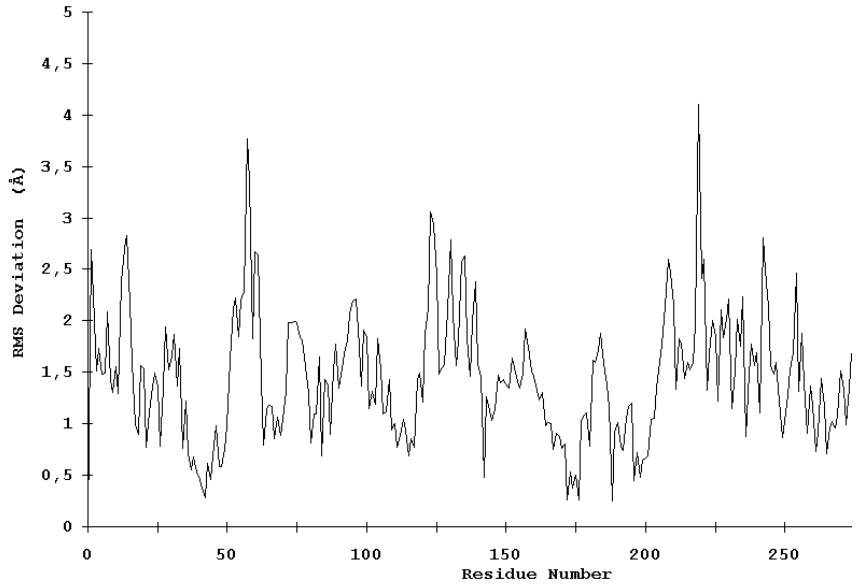

Figure 2. Root mean square deviation (RMSD) between the optimized model of MnP13-1 and the crystal structure of MnP from *P. chrysosporium*.

Modeling of MnP13-1

Taking the higher similarity scores between MnP13-1 and the reference proteins, coordinates were assigned for all the structurally conserved regions. Residues are highly conserved, with the exception of the insertions TGGN and TDSP in MnP13-1, the latter at the C-terminal. For side chain conformations exhibiting overlaping of atoms (distance between atoms < 0.8 Å), such as D48, E101, E374 and D387, alternative positions were manually assigned based on their steric feasibility. Considering 71.9 % of the residues, the RMSD from the unoptimized structure was 0.17 Å /res. After optimization, a model with a Cα deviation of 1.7 Å /res was obtained (Fig. 2). Differences in the location of Cα atoms, both in the proximal and in the distal domains were evidenced. However, the main chain fold was conserved and

it remained undistorted. Each domain seems to be more tightly packed than what it was suggested from the RMSD plot. Positions of helices B and F facing the hem group, as well as the position of the hem group itself, are highly conserved.

The TGGN sequence was modeled as a loop inserted between S231 and D232. The coordinates for this loop were obtained from the structure of 3app (acid proteinase, RMSD = 0.61 Å for last residue at previous SCR). After optimization, the extended loop translated near to S345-S347, a segment without secondary structure. The inserted G234 is hydrogen bound to E350, a residue at the preceding C-terminal loop of MnP13-1, which restrains the conformational freedom of the new loop. Large displacements are observed in residues near to this loop that could influence the Mn^{2+} binding geometry and its kinetic (see later).

Residues TDSP were constructed in extended conformation starting on A361 of the reference MnP, which determined the direction of the mainchain of the inserted residues in MnP13-1. As a result, the C-terminal of MnP13-1 emerges close to the binding site of Mn^{2+}. (Fig. 3). Two out of these four residues were found to be hydrogen bound to neighboring residues of the N-end of helix C. Hydrogen bonds between HN Q79 and OD2 D363, HN G83 and OD1 D363 and OE1 E77 and HN T362 were observed. In addition, these residues were stabilized by hydrogen bonds between themselves. P365 is at hydrogen bond distance from K180, anchoring the C-terminal to the structure of the protein.

Binding sites of Ca^{2+} and Mn^{2+}

Local optimization of ligand residues in MnP13-1, keeping fixed the ion positions, produced the bond distances shown in Table 2. At the distal side, the Ca^{2+} binding OG S91 in MnP from *P. chrysosporium* was found too far away (3.18 Å) to be a ligand in MnP13-1. In contrast, at the proximal side, O T220, OG S198 and O S198 were at 3.04 Å , 1.63 Å , and 3.06 Å , respectively, suggesting that they are Ca^{2+} ligands. The geometry of the Ca^{2+} distal binding site is certainly influenced by the replacement of P135 in MnP13-1, since HN G61 is hydrogen bound to O-P135. As a consequence, the Cα of G61 is translated 2.06 Å and the Cα of A51 is 1.67 Å closer to Ca^{2+}. In this way, O-A51 is located at the very confortable distance of 2.73 Å of Ca^{2+}, providing another possible ligand for this ion. Most of these Ca^{2+} bond distances are in good agreement with the values informed for the crystal structure of the reference MnP (Sundaramoorthy *et al.* 1994). Two water molecules are present in MnP from *P. chrysosporium* and due to the high conservation of the Ca^{2+} binding geometry, they are expected to be present in MnP13-1 as well. However, since O-A51 in MnP13-1 constitutes a better ligand than a water molecule, it is conceivable that this enzyme may contain a single water molecule at this site.

Table 2. Calcium ligands and bond distances in MnP13-1

Ligand		Distance (Å)
Ca^{2+} proximal binding site		
Thr 220 O		3.04
Asp 215 OD2		2.45
Ser 198 OG		1.63
Ser 198 O		3.06
Thr 217 OG O		2.90 2.53
Asp 222 OD1		2.55
Ca^{2+} distal binding site		
Asp 72 OD1		2.95
Gly 87 O		2.84
HOH 493		2.45
Ser 91 OG		3.18
Asp 89 OD1		2.28
HOH 545		2.40
Asp 72 O		2.61
Ala 51 O		2.73

The geometry of the Mn^{2+} binding site is highly conserved, as shown by the bond distances and side chain conformations of residues E35, E39 and D179. The optimization of this site did not produce deviations in bond distances with respect to the reference, suggesting that the Mn^{2+} binding mode and kinetic behavior of both MnPs should be very similar. Nonetheless, it should be kept in mind binding of Mn^{2+} to MnP13-1 can be influenced both by the loop TGGN inserted between S231 and D232 located below the Mn^{2+} binding site and by the inserted residues at the C-terminal end.

Aromatic binding site

An hypothetical binding site for veratryl alcohol involving residues H82, I85, E146, F148, D183, V184 and Q222 has been suggested for LiP (Poulos et al. 1993). The corresponding residues in MnP from *P. chrysosporium* are S78, N81, E143, Q145, K179, V180 and T219. Although these residues show no similarity with those of LiP, the size of the pocket allows the prediction that single ring aromatic compounds may have access to it. Residues Q79, N82, V143, Q145, K180, V181 and T219 were identified in equivalent positions in MnP13-1 model structure, which are closely related to those of the MnP reference. On the other hand, the motif L/V/I-P-X-P assigned as an aromatic binding site in peroxidases[9] is located at the left side of this putative binding site (Fig 4). I141 points to the distal side of the hem group facing H47 rather than to this site. For this reason, it is unlikely that this residue may participate in the binding of the substrate in MnP13-1 model, as it may occur in the MnP crystal structure. The next residue, P142, is located towards the hem group, unabling it as well to make contact with the aromatic substrate. Only X (E in MnP reference or V in MnP13-1) is pointing to the substrate pocket, whereas P144 ring could also help to substrate binding by Van der Waals contacts. The next residue following the numbering of this motif is Q145, which shows the overlapping of this motif with the substrate pocket described in LiP (Poulos et al. 1993).

Discussion

There is an overall similarity between the structures of MnP from *P. chrysosporium* and the one modeled for MnP13-1, as it could be predicted by the high degree of identity of their sequences. The RMSD of 1.7 Å /res is in the limit of fold conservation, although a detailed analysis of the model suggests that the main conformational changes are only related to the substitution or the insertion of residues. It is unlikely that the displacement of the main chains of the proximal and distal domains are caused by the modeling procedure employed. Instead, it is possible that they occur to improve the packing effectiveness intra domains, as it is evidenced by the low RMSD of the residues forming helices B and F, as well as of those binding the heme group. These helices contain the proximal and distal histidines, respectively.

The larger loop between S231 and S235 and the four-residues extending the C-terminal could influence the catalytic activity of the enzyme due to their close proximity to the Mn^{2+} ion site. The modeling of MnP13-1 showed that A51 is at bond distance of the Ca^{2+} ion and therefore it could be replacing a water molecule as distal ligand, thus enhancing the stability of the enzyme at high temperatures (Sutherland et al. 1997).

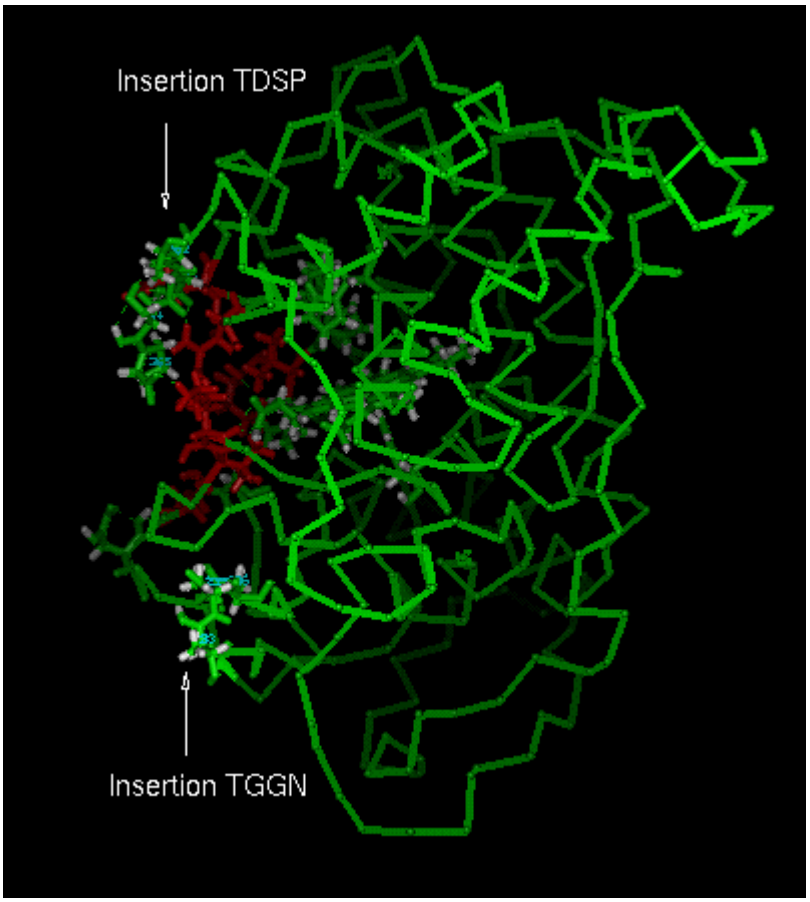

Figure 3. MnP13-1 model, highlighting the C-terminal region. The direction of the sequence TDSP at C-terminal is shown together with possible hydrogen bonds (dashed lines). Insertion of the sequence TGGN and the hydrogen bond between residues G234 and E350 at C-terminal are also shown.

Inspection for a possible aromatic binding site in MnP13-1 revealed that the geometry of the VA site assigned to LiP (Poulos et al. 1993) is very well conserved in MnP13-1, although the corresponding residues are different. The correspondence of this site between LiP and MnP is supported by the ability of some MnPs to partially oxidize veratryl alcohol in the absence of Mn^{2+} (Martinez et al. 1996, D'Annibale et al. 1996). It is interesting to note that the motif L/V/I-P-X-P described by Veitch as the aromatic binding site in peroxidases (Veitch et al. 1993) flanks this pocket in MnP13-1 (Fig 4). According to our model of MnP13-1, only V143 and P144 in this motif should contribute to binding of the substrate, since both residues point to the center of the pocket. These characteristics would imply that substrate binding to MnP13-1 should be weaker than to MnP from *P. chrysosporium*. Therefore, the ability of MnP13-1 to oxidize aromatic compounds in the absence of Mn^{2+} could be explained by the higher hydrophobicity of the putative substrate binding site due to the substitution of E143 in the MnP reference by V143 in MnP13-1.

Recently, automatic modeling procedures such as Modeler have been published, which work well in the range of 30-40% identity between sequences (Sali and Blundell, 1993). Since the identity of our sequences is over 60%, a full correspondence of our method with these procedures should be expected. On the other hand, a Ramachandran plot from the optimized model showed with more detail the conservation of same fold between MnPs from *P. chrysosporium* and *C. subvermispora* (data not shown). A

more detailed assesment of the stereochemistry such as the one implemented in Procheck (Lakowski et al, 1993) was not necessary.

Molecular modeling constitutes a powerful approach to analyze the catalytic properties of enzymes. Other authors have already utilized this tool for modeling of MnPs (Johnson et al. 1994). In this work, it has allowed us to understand the consequences of two insertions and one aminoacid substitution in MnP13-1 with respect to a reference MnP from *P. chrysosporium*. We are presently modeling another MnP isoenzyme from *C. subvermispora* which exhibits different catalytic properties than those of MnP13-1.

Acknowledgments

This work was supported by grants 4533 from Universidad de Concepción and 1971239 from FONDECYT

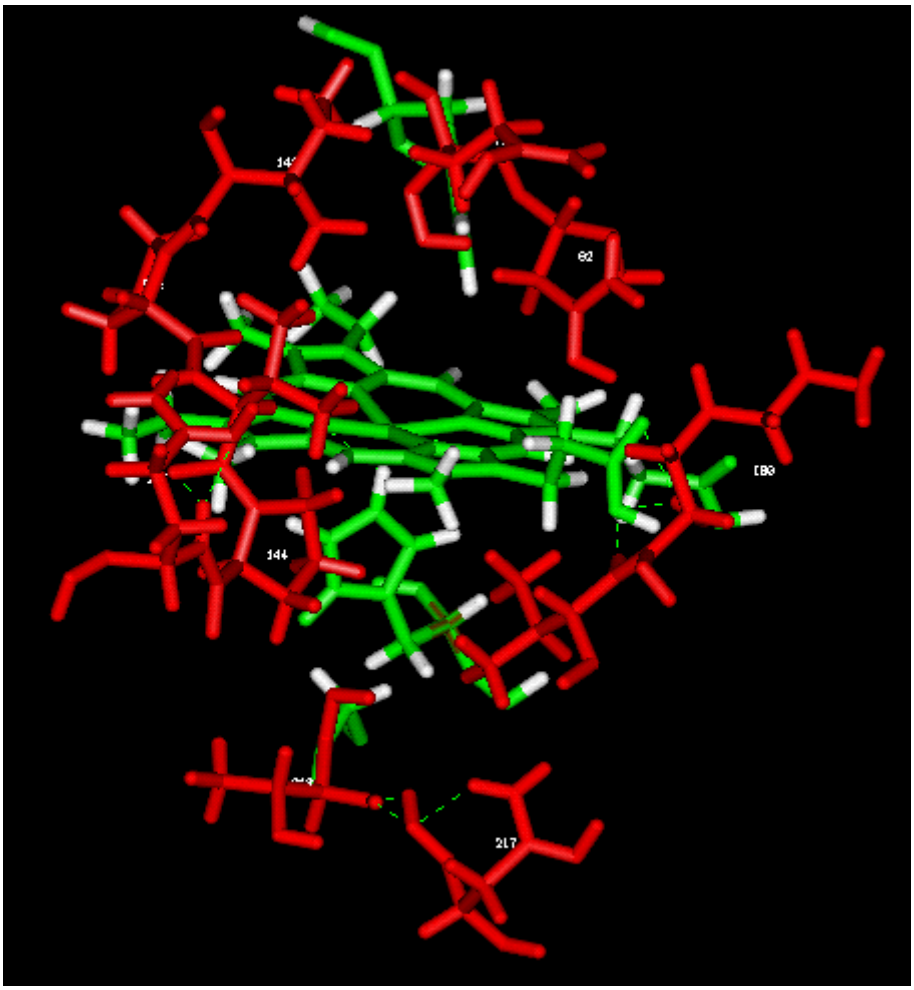

Figure 4. Substrate binding pocket in MnP13-1. Residues I141, P142, V143 and P144 constitute the motif described by Veitch (Veitch 1993). Residues showing the side chains are those of the veratryl binding pocket in LiP according to Poulos (Poulos et al. 1993). Dashed lines represent hydrogen bonds.

References

Alic, M., Akileswaran, L. and Gold, M. H. (1997) Characterization of the gene encoding manganese peroxidase isozyme 3 from *Phanerochaete chrysosporium*. Biochimica et Biophysica Acta 1338: 1-7.

Blanchette R.A., Burnes T.A., Eerdmans M.M., Akhtar M., (1992) Evaluating isolates of *Phanerochaete chrysosporium and Ceriporiopsis subvermispora* for use in biological pulping processes. Holzforschung 46:106-115.

Blundell ,T. L., Sibanda, B.L., Sternberg, M.J.E., Thornton, J. M., (1987) Knowledge-based prediction of protein structures and the design of novel molecules, Nature 326, 347-352.

D'Annibale A., Crestini C., Di Mattia E., Giovannozzi-Sermanni G. (1996) Veratryl alcohol oxidation by manganese-dependent peroxidase from *Lentinus edodes*. Journal of Biotechnology 48: 231-239.

Edwards, S. L., Raag, R., Wariishi, H., Gold, M. H. and Poulos, T. L. (1993) Crystal structure of lignin peroxidase. Proceedings of the National Academy of Sciences USA 90: 750-754.

Greer, J. (1981) Comparative Model-building of the Mammalian Serine Proteases, Journal of Molecular Biology 153, 1027-.

Henrissat, B., Saloheimo, M., Lavaitte, S. and Knowles, K.C. (1990) Structural Homology Among the peroxidase Enzyme

Family Revealed by Hydrophobic Cluster Analysis, Proteins 8: 251-257.

Johnson, F., Loew, G. H. and Du, P. (1994) Homology models of two isozymes of manganese peroxidase: predicion of Mn (II) binding site. Proteins 20: 312-319.

Kunishima, N., Fukuyama, K., Matsubara, H., Hatanaka, H., Shibano, Y. and Amachi, T. (1994) Crystal structure of the fungal peroxidase from *Arthromyces ramosus* at 1.9 Å resolution. Journal of Molecular Biology 235: 331-344.

Lakowski, R. A., MacArthur, M. W., Moss, D. S. and Thornton, J. M. (1993), PROCHECK: a program to check the stereochemical quality of protein structures, Journal of Applied Crystallography, 26, 283-291.

Lobos, S., Larrain, J., Salas, L., Cullen, D. and Vicuña, R. (1994) Isoenzymes of manganese-dependent peroxidase and laccase produced by the lignin-degrading basidiomycete *Ceriporiopsis pubvermispora*. Microbiology 140: 2691-2698.

Martinez, M. J., Ruiz-Duenas, F. J., Guillen F., Martinez, A. T. 1996, Purification and catalytic properties of two manganese peroxidase isoenzymes from *Pleurotus eryngii* European Journal of Biochemistry 237: 424-432.

Mayfield, M. B., Godfrey, B. J. and Gold, M. H. (1994) Characterization of the Mn^{2+} gene encoding manganese peroxidase isozyme 2 from the basidiomycete *Phanerochaete chrysosporium*. Gene 142: 231-235.

Needleman, S. B., Wunsch, C.D. 1970, A General Method Applicable to the Search for Similarities in the Amino Acid Sequence of Two Proteins, Journal of Molecular Biology 48, 443-453.

Otjen L., Blanchette R., Effland M., Leatham G. 1987. Assesment of 30 white-rot basidiomycetes for selective lignin degradation. Holzforschung 41:343-349.

Pearlman, D. A., Case, D. A., Caldwell, J. C., Seibel, G. L., Singh, U. Ch., Weiner, P., Kollman, P. A. (1991), AMBER 4.0, University of California, San Francisco.

Poulos, T. L., Edwards, S. L., Wariishi, H. and Gold, M. H. (1993) Crystallographic refinement of lignin peroxidase at 2 Å. Journal of Biological Chemistry 268: 4429-4440.

Pribnow, D., Mayfield, M. B., Nipper, V. J., Brown, J. A. and Gold, M. H. (1989) Characterization of a DNA encoding a manganese peroxidase from the lignin-degrading bacidiomycete *Phanerochaete chrysosporium*. Journal of Biological Chemistry 264: 5036-5040.

Salas, C., Lobos, S., Larraín, J., Salas, L., Cullen, D. and Vicuña, R. (1995) Properties of laccase isoenzymes produced by the bacidiomycete *Ceriporiopsis subvermispora*. Biotechnology and Applied Biochemistry 21: 323-333.

Sali, A. and Blundell, T.L. (1993) Comparative protein modelling by satisfaction of spatial restraints. Journal of Molecular Biology 234: 779-815

Sundaramoorthy, M., Kishi, K., Gold, M. H. and Poulos, T. L. (1994) The crystal structure of manganese peroxidase from *Phanerochaete chrysosporium* at 2.06-angstrom resolution. Journal of Biological Chemistry 269: 32759-32767.

Sutherland, G. R. J., Zapanta, L.S., Tien, M. and Aust, S. D. 1997, Role of calcium in maintaining the heme environment of manganese peroxidase. Biochemistry 36: 3654-3662

Urzúa U, Larrondo L. F., Lobos S., Larraín J., Vicuña R. 1995. Oxidation reactions catalyzed by manganese peroxidase isoenzymes from *Ceriporiopsis subvermispora*. FEBS Letters 371: 132-136.

Veitch NC. 1993. Plant Peroxidases in Biochemistry and Physiology. K. G. Welinder, S. K., Rasmussen, C. Penel, and H. Grepin, eds., University of Geneva.